these differences is probably the disulphide bond between the light chains in Dob and Mcg, which is not present in the HM-1 molecule.

Hinge-deleted molecules such as m0, lack disulphide bonds between the heavy chains. The C_H2 domains will therefore drift apart because there are no transinteractions between these domains[17,18] (Fig. 2*a*). As a result, the Clq-binding sites on the two C_H2 domains will be dislocated and may even be distorted. Because Clq is multivalent in its binding to IgG, tight cooperative binding between IgG and Clq may be impossible for the m0 molecule. The only difference between m0 and HM-1 is in the ability of HM-1 to form a disulphide bond between its heavy chains. Thus in complement activation the major role of the hinge seems to be covalent linking of the heavy chains.

It has been difficult to crystallize intact active IgG molecules for X-ray diffraction analysis because of the flexible hinge region. The mutant HM-1 is likely to be rigid, therefore it may be a good candidate for X-ray analysis of an intact, functionally active IgG molecule.

Note added in proof: We have recently shown that HM-1 promotes phagocytosis mediated by FcRI with high efficiency, but m0 is negative[25]. Thus, bridging of the heavy chains is also a prerequisite for efficient FcR signalling, whereas Fab arm flexibility and distance between Fab and Fc seem not to be necessary. □

Received 9 November 1992; accepted 5 April 1993.

1. Feinstein, A., Richardson, N. & Taussig, M. J. *Immun. Today* **7**, 169–174 (1986).
2. Sandlie, I, Aase, A., Westby, C. & Michaelsen, T. E. *Eur. J. Immun.* **19**, 1599–1603 (1989).
3. Dangl, J. L. *et al. EMBO J.* **7**, 1989–1994 (1988).
4. Duncan, A. R. & Winter, G. *Nature* **332**, 738–740 (1988).
5. Nezlin, R. *Adv. Immun.* **48**, 1–40 (1990).
6. Burton, D. R. *Molec. Immun.* **22**, 161–206 (1985).
7. Michaelsen, T. E., Aase, A., Westby, C. & Sandlie, I. *Scand. J. Immun.* **32**, 517–528 (1990).
8. Norderhaug, L. *et al. Eur. J. Immun.* **21**, 2379–2384 (1991).
9. Tan, L. K., Shopes, R. J., Oi, V. T. & Morrison, S. L. *Proc. natn. Acad. Sci. U.S.A.* **87**, 162–166 (1990).
10. Klein, M. *et al. Proc. natn. Acad, Sci. U.S.A.* **78**, 524–528 (1981).
11. Deutsch, H. F. & Suzuki, T. *J. Immun.* **107**, 929–930 (1971).
12. Marquart, M., Deisenhofer, J. & Huber, R. *J. molec. Biol.* **141**, 369–391 (1980).
13. Ito, W. & Arata, Y. *Biochemistry* **24**, 6467–6474 (1985).
14. Rajan, S. S. *et al. Molec. Immun.* **20**, 787–899 (1983).
15. Silverton, E. W., Navia, M. A. & Davies, D. R. *Proc. natn. Acad. Sci. U.S.A.* **74**, 5140–5144 (1977).
16. Schneider, W. P., Wensel, T. G., Stryer, L. & Oi, V. T. *Proc natn. Acad. Sci. U.S.A.* **85**, 2509–2513 (1988).
17. Michaelsen, T. E. *Scand. J. Immun.* **5**, 1123–1128 (1976).
18. Seegan, G. W. *et al. Proc. natn. Acad. Sci. U.S.A.* **76**, 907–911 (1979).
19. Kunkel, T. A., Roberts, J. D. & Zakour, R. A. *Meth. Enzym.* **154**, 367–382 (1987).
20. Sanger, F., Nicklen, S. & Coulson, A. R. *Proc. natn. Acad. Sci. U.S.A.* **74**, 5463–5467 (1977).
21. Neuberger, M. S. *et al. Nature* **314**, 268–270 (1985).
22. Potter, H., Weir, L. & Leder, P. *Proc. natn. Acad. Sci. U.S.A.* **81**, 7161–7165 (1984).
23. Neuberger, M. S. *EMBO J.* **2**, 1373–1378 (1983).
24. Laemmli, U. K. *Nature* **227**, 680–685 (1970).
25. Aase, A., Sandlie, I., Norderhaug, L., Brekke, O.H. and Michaelsen T.E. Eur J. Immunol., (in the press).

ACKNOWLEDGEMENTS. We thank M.-P. Lefranc for the Cγ3 gene, M. Neuberger for the pSV2gpt V_{NP} vector and P. Hudson for comments on the manuscript. This work was supported by a grant from The Norwegian Research Council for Science and Humanities.

Segmental organization of embryonic diencephalon

Michael C. Figdor*† & Claudio D. Stern‡§

* Institute of Histology and Embryology, Schwarzspanierstrasse 17, 1090 Vienna, Austria
‡ Department of Human Anatomy, University of Oxford, South Parks Road, Oxford OX1 3QX, UK
† Present address: Beckman Institute, California Institute of Technology, Pasadena, California 91125, USA.

THE diencephalon is a complex integration centre and intricate relay station of the vertebrate brain[1–3]. Its development involves the generation of great cellular diversity and neuronal specificity. We report here that it becomes organized in steps, through a stereotyped sequence of neuromeric subdivisions. Diencephalic neuromeres define four cellular domains (D1–D4) that can be followed throughout development, each unit contributing to a well defined part of the adult structural pattern. We propose that the segmental identity of each diencephalic unit is specified by a unique combination of genes[4–13], maintained by polyclonal cell lineage restrictions. A comparison of vertebrate and arthropod development suggests that the basic principles that control anterior axial patterning and set up neuronal specificity in the embryonic central nervous system are highly conserved in evolution.

Many morphological studies have been done[14–21] to determine the basic units of pattern formation in the forebrain, but they have come to irreconcilable conclusions. We have now studied the development of the embryonic diencephalon of the chick embryo by scanning electron microscopy (SEM). A pattern of transverse furrows and ridges is seen, repeated along the anteroposterior axis of the third ventricle (Fig. 1*a*). Four regions can be distinguished, which we designate as neuromeres D1–D4, numbered in anterior-to-posterior sequence. The borders between neuromeres appear as ridges, subdividing the otherwise smooth relief of the third ventricle. They form in precise temporal sequence (D4/M: stage-12 (ref. 22); D1/D2:

§ To whom correspondence should be addressed.

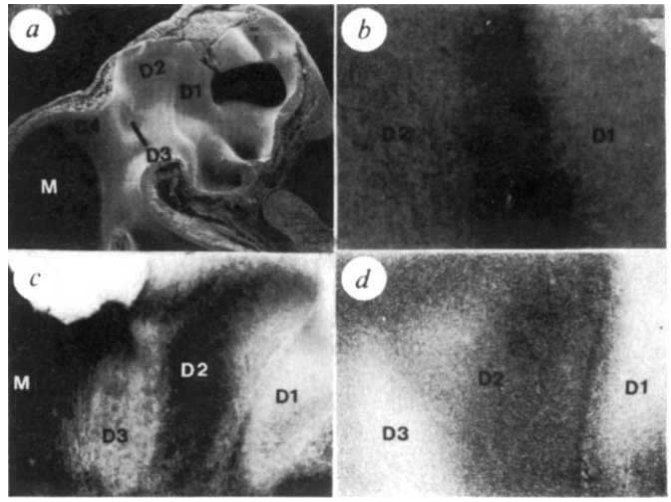

FIG. 1 Morphology of diencephalic neuromeres and alternating patterns revealed by antibodies. *a*, SEM of stage-24[22] chick embryo in medial view. *b*, NCAM is accumulated at neuromere boundaries: the border between D1 and D2 stains intensely. Whole mount of stage-24[22] embryo. Acetylcholinesterase activity (*c*) and peanut agglutinin (*d*) reveal an alternating pattern of staining: even-numbered neuromeres show high levels of activity. In D4, the development of the early tract of the posterior commissure (TPC axons) is seen (*c*), restricted at both anterior and posterior boundaries of D4. Whole mount of stage-25[22] embryo. D1–D4, diencephalic neuromeres. T, telencephalon. M, mesencephalon.
METHODS. For SEM, chick embryos at stages 12–39[22] were explanted in PBS, pH 7.4 at 4°C and the brain bisected. They were fixed for 1–3 h in 2% paraformaldehyde, 2.5% glutaraldehyde and 0.025% $CaCl_2$ in 0.1 M cacodylate buffer (pH 7.4). After several washes in this buffer, they were incubated for 1 h in 2% OsO_4, washed in cacodylate buffer, dehydrated, transferred to acetone and critical-point dried overnight. Specimens were mounted on stubs, sputter coated (Nanotech SEM Prep 2, 4 min) and viewed with a Philips SEM 515. Antibody, cholinesterase and lectin histochemistry were done by previously described techniques[23–25]. Anti-NCAM antibody was a gift of Dr U. Rutishauser.

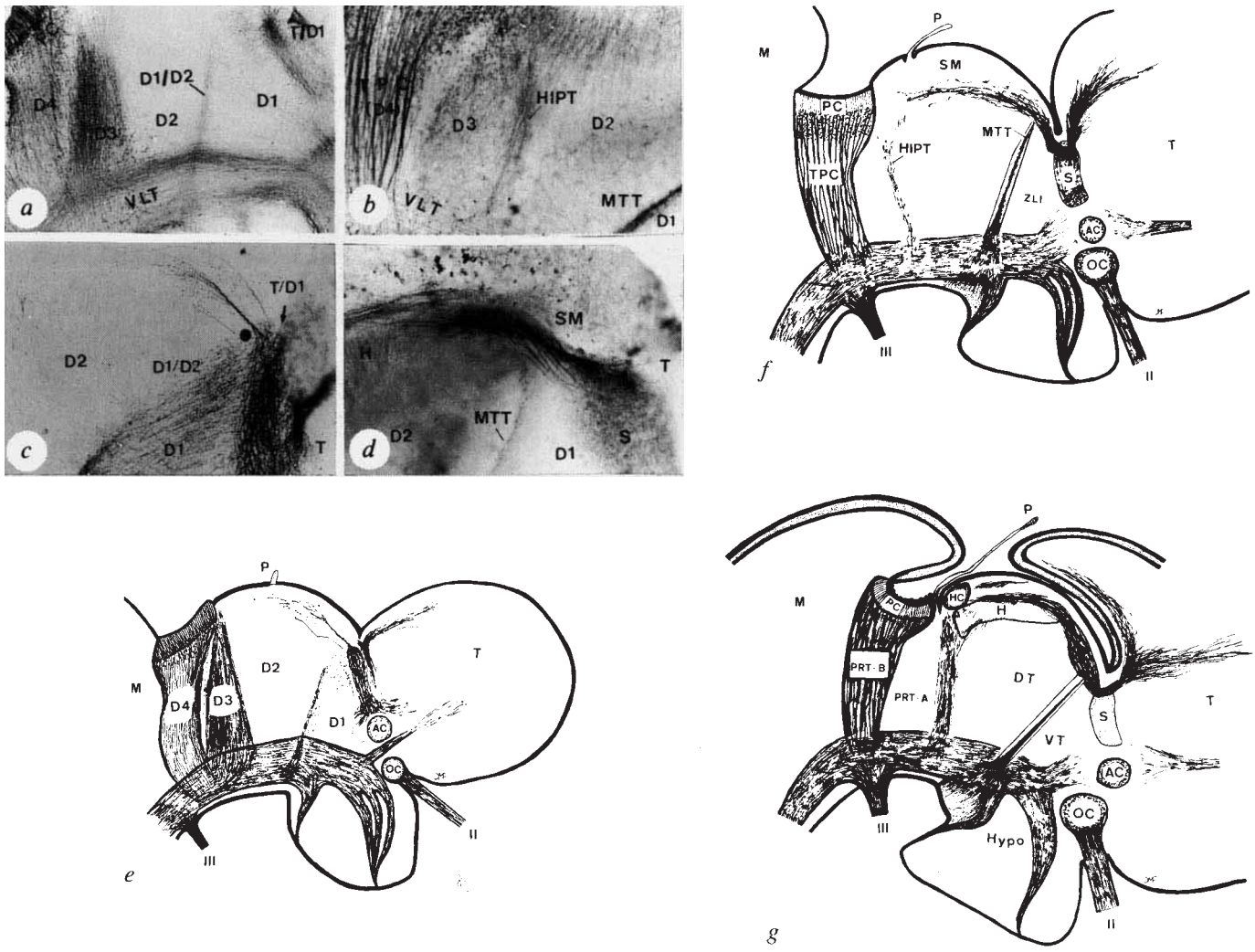

FIG. 2 Development of the segmental scaffold of primary axon fascicles in the embryonic chick diencephalon, visualized in whole mounts with an antibody against neurofilament-associated proteins[37]. *a*, Stage-27[22]. D4 can be defined by the formation of the posterior commissure (PC) and its tract (TPC). D3 contains a population of axons, constrained by both boundaries of D3. D2 is limited anteriorly by an axon fascicle, the presumptive mamillothalamic tract (MITT), developing in the ZLI. *b*, The D1/D2 pathway forms a barrier respected by D1 axons. Stage 25. Individual D1 axons change their direction locally by 90° along the T/D1 border, starting to fasciculate with each other at the D1/D2 border. A small set of primary stria medullaris (SM)-axons changes its direction abruptly at the dorsal margin of the T/D1 border (circle). Leading SM-axons seem to pioneer as individuals, forming a fan of very fine axonal processes. *c*, *d*, The adult organization of diencephalic connectivity develops from the primary neuromeric scaffold. Stage 40[22]. The pattern of major diencephalic axon tracts and commissures forms by addition of a large number of axons onto the primary axonal scaffold. D4 can be defined by the selective fasciculation of TPC-axons to form thick cables, characteristic of the adult. Anteriorly (*d*), the septal region (S) can be seen to develop from the early T/D1 border. D2 axons originating from the habenula (H) grow posteriorly, forming the D2/D3 fascicle (HIPT, *c*). *e*, Stage-27[22]; *f*, stage-30[22]; *g*, stage-40[22]. The pineal (P), arising anterodorsally in D2, gradually shifts posteriorly to the point where the D2/D3 and D3/D4 borders abut, thus separating the habenular commissure (HC) from PC. II, Optic nerve; III, exit point of oculomotor nerve; AC, anterior commissure; OC, optic chiasm and associated commissures; DT, dorsal thalamus; VT, ventral thalamus; Hypo, hypothalamus; PRT-A, -B, anterior and posterior parts of pretectum. METHODS. Binding of monoclonal antibody 3A10[37] was visualized by immunoperoxidase histochemistry as described in Fig. 1.

stage-14 (ref. 22); T/D1: stage-15 (ref. 22); D3/D4: stage-16 (ref. 22); D2/D3: stage-17 (ref. 22) and have characteristic shapes and sizes: even-numbered neuromeres are broad dorsally, odd neuromeres are broad ventrally.

Localization of the neural cell adhesion molecule (NCAM), acetylcholinesterase (AChE) activity and peanut agglutinin (PNA) binding demonstrates differences in the morphological pattern: NCAM is concentrated at the D1/D2 boundary (Fig. 1*b*). AChE (Fig. 1*c*) and PNA-binding (Fig. 1*d*) reveal an alternating pattern: the reactions are intense in even-numbered neuromeres and weak in odd-numbered ones. These patterns are interesting because in other embryonic regions (somite halves[23], rhombomeres[24,25] and barrel fields in the somatosensory cortex[26]) NCAM, cholinesterase and PNA-receptors may be used to define morphogenetic units.

How does this simple metameric pattern correspond to the complex organization of the adult diencephalon? Following the pattern of axonal differentiation continuously during development demonstrates that the basic organization of diencephalic axonal connectivity is established by stereotypic addition of large numbers of axons onto a simple grid of primary fascicles. A direct correspondence is seen between the early neuromeric pattern and the adult structural pattern (Fig. 2).

A small number of embryonic axons appears at invariant positions within the embryonic chick forebrain, using neuromere boundaries to navigate, forming a well defined set of adult

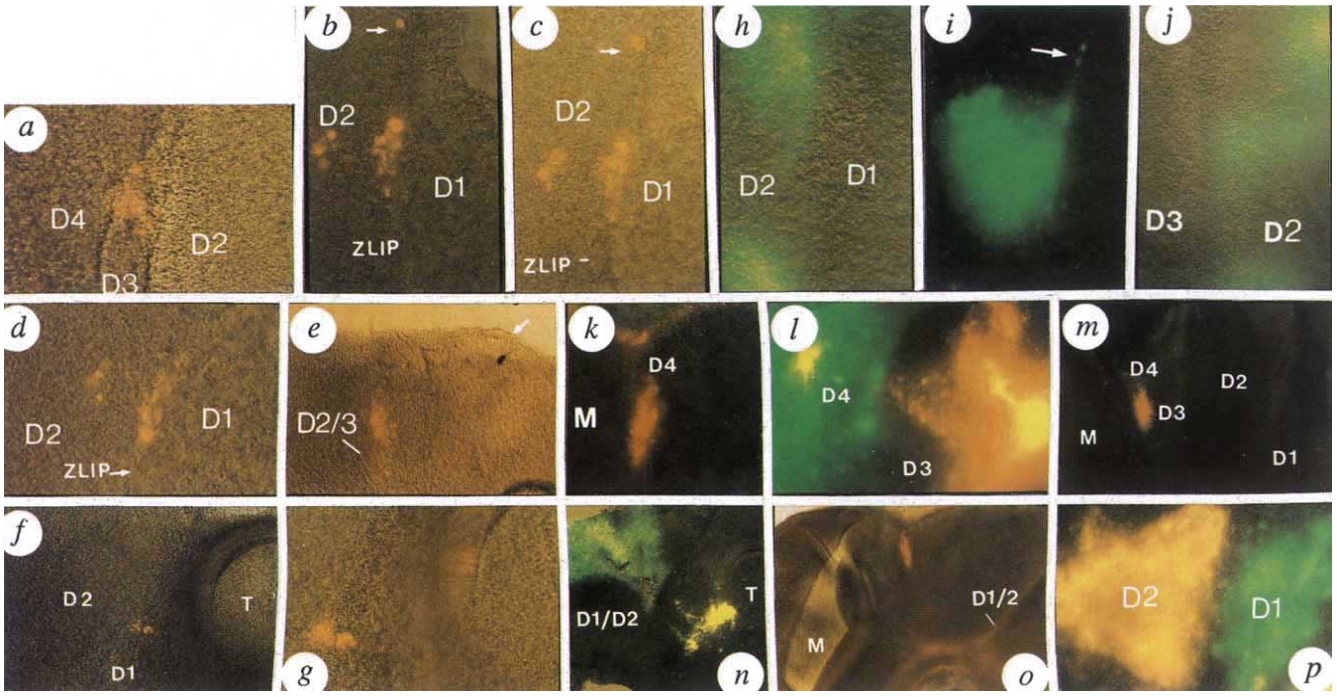

FIG. 3 Neuromere boundaries represent borders of polyclonal lineage restriction, demonstrated by intracellular injection of lysine-rhodamine-dextran (LRD) into single cells (*a–g*) and by labelling with carbocyanine dyes (*h–p*). *a–g*, Results from single cell injection of LRD into 318 stages 15–21[22] embryos. Clones varied in size from a few cells to up to 600 and spanned up to 300 μm. At stage-17[22], D1 and D3 measure 150 μm at their longest point, D2 extends over 500 μm, and D4 is 250 μm long. From the extent of the clones in each neuromere we calculated the probability that the lineage restrictions are due to chance. In injections before stage-10, clones frequently cross neuromere boundaries (χ^2 2.03, 1 d.f.; $P>0.1$). By contrast, clones generated after stage-17 never cross ($\chi^2=19.0$, 1 d.f.; $P<0.001$). *a*, 32-cell clone (labelled at stage-19[22]), restricted at both boundaries of D3, spanning the whole width of the neuromere. *b*, *c*, Part of this 26-cell clone (injected stage-18[22]) is located within the D1/D2 boundary. Despite extensive dorsoventral spread (one cell (arrow) can be seen nearly at the dorsal midline), the clone does not enter D1. The photographs are taken at different focal planes. *d*, 60-cell clone (injected at stage-16[22]) aligned along D1/D2 boundary. *e*, >200-cell, D-shaped clone at the D2/D3 boundary (stage-18[22] injection). Arrow, pineal gland. *f*, *g*, Stage-15[22] injection. Labelled cells are in two main groups, each restricted by one of the boundaries of D1. *h*, *p*, Labelled cells resulting from 279 focal injections of carbocyanine dyes (DiI, red and DiO, green) into the forebrain (stages 14–23[22]). *h*, Labelled cells restricted at the D1/D2 boundary. *i*, Both boundaries of D2 are respected, and there is extensive spread of labelled cells along the D1/D2 boundary (arrow). *j*, Labelled progeny of an injection at stage-16[22], restricted at the D2/D3 boundary. *k*, DiI injection targeted at the D4/M border; labelled cells almost fill the neuromere but do not cross into either D3 or the midbrain. *l*, Injection of DiI (D3) and DiO (D4), showing considerable spread within each neuromere but neither crosses the boundary. The D4 group aligns along the border. *m*, DiI injection (stage-18[22]). Labelled cells are restricted to D4. *n*, DiI injection into the anterior forebrain and DiO into posterior forebrain (early stage-14[22] embryo), showing considerable spread within D1, with a few cells reaching the D1/D2 border. In the posterior forebrain, DiO-labelled cells are only restricted at the DS1/D2 boundary; they spread extensively posterior to this border. At stage-14[22], only the D1/D2 and D4/M boundaries have formed. Labelled cells have therefore spread across the T/D11 (DiI) and D2/D3 (DiO) boundaries. *o*, Two separate DiI injections (stage-18[22]): the posterior one gave rise to cells restricted to D4. The anterior injection generated labelled primary axons at the D1/D2 boundary. *p*, DiI injection into D1 and DiO into D2 (stage-16[22]). Labelled cells reach the D1D2 border but do not intermix.

METHODS. LRD[29–30] (10 mg ml^{-1}) was injected *in ovo*, essentially as described previously[29,30]. Filled electrode impedance was 60–100 MΩ. Embryos were fixed after 36–48 h reincubation. 3,3'-Dioctadecyl indocarbocyanine perchloride (DiI) or 3,3'-dioctadecyloxacarbocyanine perchlorate (DiO) (Molecular Probes) were injected by air pressure *in ovo*. Embryos were fixed after 48–72 h incubation.

axon tracts and commissures that is highly conserved during vertebrate evolution[1–3,14,15], each structural element separating the major diencephalic regions of the adult. Diencephalic neuromere borders therefore appear to be a conserved scaffold of pre-existing, region-specific axon pathways in the early forebrain neuroepithelium. This is similar to the development of the central nervous system (CNS) in arthropods, which is established on a simple segmental plan[27,28]: the growth cones of early pioneer neurons of insects use positional cues within the neuroepithelium, making cell-specific choices at local decision regions to set up a stereotyped, orthogonal scaffold of axon fascicles, repeated at each embryonic segment. Later-developing axons grow along this basic framework, each choosing uniquely 'labelled' axon-pathways on which they selectively fasciculate.

If segmentation of the diencephalon is important for pattern formation, then an effective mechanism must preserve the autonomy of the individual units: unrestrained cell mixing across segment boundaries would destroy the metameric pattern. We used two different approaches to test whether diencephalic neuromere boundaries represent barriers to the mixing of cells. First, we injected a fluorescent lineage tracer[29,30] into a single neuroepithelial cell. Clones generated from injections made before formation of neuromere borders (stages 6–12, ref. 22) often crossed into the adjacent neuromere. In contrast, all clones generated from injections made after border formation failed to spread into the adjacent neuromere (Fig. 3 *a–g*). In some cases, especially in D3, whose anterior and posterior borders are very close (Fig. 3*a*), the clone abutted two borders and respected both. Clones were unable to cross the boundaries despite their extensive spread in other directions (Fig. 3*b–g*) and their large size, and were often aligned along the adjacent border (Fig. 3*b–e*). Within the limits of individual diencephalic neuromeres, labelled and unlabelled cells were intermixed

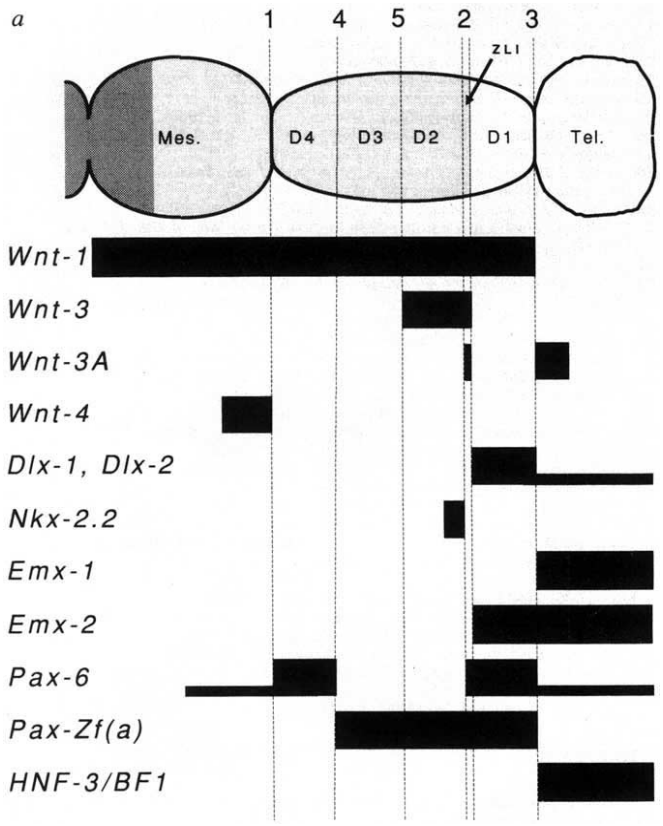

(b)

Early diencephalic neuromeres and their boundaries

Neuromeres and their boundaries	Adult structures
Telencephalon/D1 (T/D1) boundary	Septum verum (S) Septum pellucidum (mammals) Anterior commissure (AC) Anterior pallial commissure (APC) (corpus callosum of mammals) Posterior pallial commissure (PPC) (hippocampal commissure) Fornix Optic chiasm (OC)
D1	Ventral thalamus (VT) Hypothalamus (Hypo)
D1/D2 boundary	Zona limitans intrathalamica (ZLI) Mamillothalamic tract (MTT)
D2	Dorsal thalamus (DT) Habenula (H) Stria medullaris (SM)
D2/D3 boundary	Habenulo-interpeduncular tract (HIPT) Habenular commissure (HC) Pineal gland (P)
D3	Anterior part of pretectum (PRT-A) (excluding PC and TPC)
D3/D4 boundary	Anterior border of posterior commissure (PC) and its associated tract (TPC)
D4	PC + TPC-containing part of pretectum (posterior part of pretectum; PRT-B)
D4/midbrain boundary (D4/M)	Posterior border of PC + TPC Anterior border of tectal commissure Exit point of oculomotor nerve (III)

FIG. 4 *a*, Expression domains (shown as black horizontal bars) of 12 putative regulatory genes[5–13] from mouse, zebrafish and frog that respect diencephalic neuromere boundaries. Boundaries were defined by the morphological studies described above and using the position of axon fascicles (Fig. 2) as landmarks to reinterpret the published domains of expression of these genes. In the mouse, diencephalic neuromeres appear at 9–11 days postcoitum (p.c.) and are comparable to their chick counterparts (unpublished observations). The diagram also shows the region (light shading) competent to express the *engrailed* homologue, *En-2*, on grafting of mesencephalic neuroepithelium[36] and the region that normally expresses *En-2* (dark shading). The numbers above the diencephalic neuromere boundaries correspond to the order in which these borders form during development. *b*, Correspondence between early diencephalic neuromeres and their boundaries and the adult structures that form in them. This correspondence was used to relate the expression domains of individual genes to the neuromeric pattern.

extensively (Fig. 3*b–g*), showing no tendency to align or disperse in any direction. This suggests that the early embryonic diencephalon is not further subdivided by a set of hidden boundaries.

Second, we marked small groups of cells within diencephalic neuromeres, using targeted microinjections of carbocyanine dyes. This allowed us to demonstrate directly that adjacent groups of cells do not mix across an intervening neuromere boundary. The results confirm those obtained by intracellular injection (Fig. 3*h–p*): the progeny of cells labelled after border formation fails to cross any of the borders encountered. Injections often produced progeny that filled the entire neuromere with labelled cells, challenging both boundaries (Fig. 3*i*,*k*,*p*).

Both experiments demonstrate that diencephalic neuromeres represent discrete units of polyclonal lineage restriction, like other segmented structures in the vertebrate embryo (somites[29,31], hindbrain[30]). In insects, holyclonal lineage restrictions have been suggested to define developmental compartments, each comprising "all the surviving descendants of a small group of founder cells, which respects defined spatial boundaries"[32,33]. These boundaries could act to define the limits of autonomous units of pattern formation, ". . . the animal being made in modules, each growing and shaping itself independently of the others and each being subject to somewhat independent genetic control"[33].

In both insects and vertebrates, the head appears to be subdivided into two segmented regions. Posterior (gnathal in insects, hindbrain in vertebrates) segments are specified by a combinatorial code of gene expression that continues into the trunk (Hox code[34]). Recent results[10,35] suggest that the anterior segments of both (cephalic in insects, forebrain/midbrain in vertebrates), which contain the higher integration centres, seem to use a fundamentally different code. The development of a highly conserved set of invariant reference points in the vertebrate forebrain, derived from the early metameric pattern (Figs 1*a*, 2 and 4*b*) allows us to interpret the domains of gene expression described in this region. Several putative regulatory genes are restricted at diencephalic neuromere boundaries (Fig. 4).

A recent experiment in the chick embryo[36] demonstrated that the potential of the anterior neural tube to express *Engrailed-2 (En-2)* and to develop mesencephalic fates stops sharply at the zona limitans intrathalamica (ZLI), which our results reveal to be derived from the earliest developing intraprosencephalic neuromere border (D1/D2). Thus, an early step in pattern formation of the vertebrate forebrain may be the segregation of two supra-segmental polyclones of founder cells, each displaying a fundamentally different cell state: an anterior one (T+D1), incompetent to express *En-2* and lacking mesencepha-

lic potential, and a posterior one (D2+D3+D4), competent to express *En-2*, and able to develop mesencephalic fates.

In *Drosophila*, interactions between cells expressing the segment polarity genes *wingless* (*wg*) and *engrailed* (*en*) are required to set up and to pattern segmental units by controlling the expression of other genes, such as the homeobox gene *distal-less* (*dll*)[35]. In vertebrates, the border of expression of two homologues of *wg*, *Wnt-3* and *Wnt-3A* (ref. 5) not only coincides with the same diencephalic neuromere border (D1/D2;ZLI) where *En-2* competence stops, but also abuts directly with the expression domains of several members of the *Dlx* multigene family, the vertebrate homologues of *dll* (refs 7, 9). Thus, in both arthropods and vertebrates, the same genes could be used not only to pattern segmental units in anterior regions of the head, but also to set up a simple system of local positional cues and uniquely labelled pathways, required by growth cones to navigate selectively within the embryonic CNS. □

Received 30 December 1992; accepted 5 April 1993.

1. Ramón y Cajal, S. *Studies on the Diencephalon* (Thomas, Springfield, 1966).
2. Ariëns Kappers, C. U., Huber, G. C. & Crosby, E. C. *The Comparative Anatomy of the Nervous System of Vertebrates, Including Man* (Hafner, New York, 1960).
3. Sarnat, H. B. & Netsky, M. G. *Evolution of the Nervous System* (Oxford Univ. Press, Oxford, 1981).
4. Wilkinson, D. G., Bailes, J. A. & McMahon, A. P. *Cell* **50**, 79–88 (1987).
5. Roelink, H. & Nusse, R. *Genes Dev.* **5**, 381–388 (1991).
6. McGrew, L. L. Otte, A. P. & Moon, R. T. *Development* **115**, 463–473 (1992).
7. Price, M. *et al. Nature* **351**, 748–751 (1991).
8. Price, M. *et al. Neuron* **8**, 241–255 (1992).
9. Porteus, M. H. *et al. Neuron* **7**, 221–229 (1991).
10. Simeone, A. *et al. Nature* **358**, 687–690 (1992).
11. Walther, C. & Gruss, P. *Development* **113**, 1435–1449 (1991).
12. Krauss, S. *et al. Nature* **353**, 267–270 (1991).
13. Tao, W. & Lai, E. *Neuron* **8**, 957–966 (1992).
14. Kuhlenbeck, H. *The Central Nervous System of Vertebrates* (S. Karger, Berlin, 1973).
15. von Kupffer, K. in *Handbuch der vergleichenden und experimentellen Entwicklungslehre der Wirbeltiere.* (ed. Hertwig, O.). Bd 2, Teil 3 (Fischer, Jena, 1906).
16. Rendahl, H. *Acta zool.* **5**, 119–344 (1924).
17. Bergquist, H. *Progr. Brain Res.* **5**, 223–229 (1964).
18. Vaage, S. *The Segmentation of the Primitive Neural Tube in Chick Embryos* (Gallus domesticus) (Springer, Berlin, 1969).
19. Keyser, A. *Acta anat.* **83** (suppl. 59), 1–177 (1972).
20. Puelles, L., Amat, J. A. & Martinez-de-la-Torre, M. *J. comp. Neurol.* **266**, 247–268 (1987).
21. Altman, J. & Bayer, S. A. *J. comp. Neurol.* **275**, 346–405 (1988).
22. Hamburger, V. & Hamilton, L. *J. Morph.* **88**, 49–92 (1951).
23. Stern, C. D., Sisodiya, S. M. & Keynes, R. J. *J. Embryol. exp. Morph.* **91**, 209–226 (1986).
24. Lumsden, A. & Keynes, R. *Nature* **337**, 424–428 (1989).
25. Layer, P. G. & Alber, R. *Development* **109**, 613–624 (1990).
26. Cooper, N. G. F. & Steindler, D. A. *J. comp. Neurol.* **249**, 157–169 (1986).
27. Bate, C. M. & Grünewald, E. B. *J. Embryol. exp. Morph.* **61**, 317–330 (1981).
28. Thomas, J. B. *et al. Nature* **310**, 203–207 (1984).
29. Stern, C. D. *et al. Development* **104** (suppl.), 231–244 (1988).
30. Fraser, S., Keynes, R. & Lumsden, A. *Nature* **344**, 431–435 (1990).
31. Stern, C. D. & Keynes, R. J. *Development* **99**, 261–272 (1987).
32. Garcéia-Bellido, A., Ripoll, P. & Morata, G. *Nature New Biol.* **245**, 251–253 (1973).
33. Lawrence, P. A. *Nature* **344**, 382–383 (1990).
34. McGinnis, W. & Hoxlauf, R. *Cell* **68**, 283–302 (1992).
35. Cohen, S. M. & Jürgens, G. *Nature* **346**, 482–485 (1991).
36. Martínez, S., Wassef, M. & Alvarado-Mallart, R. M. *Neuron* **6**, 971–981 (1991).
37. Yamada, T. *et al. Cell* **64**, 635–648 (1991).

ACKNOWLEDGEMENTS. We thank M. Lomas for help with electron microscopy, M. Bronner-Fraser, S. E. Fraser, R. W. Guillery, R. J. Keynes, R. Krumlauf, J. H. Lewis, A. R. G. S. Lumsden and A. P. McMahon for valuable comments on the manuscript and advice and E. Boncinelli, D. Duboule, S. Krauss, N. Papalopulu and P. Salinas for unpublished information. M.C.F. received an Auslandsstipendium from B.M.W.F. (Austria). C.D.S. is supported by MRC, SERC and the Wellcome Trust.

Protein kinase C is required for light adaptation in *Drosophila* photoreceptors

R.C. Hardie*, A. Peretz†, E. Suss-Toby†, A. Rom-Glas†, S. A. Bishop*, Z. Selinger‡ & B. Minke†§

* Department of Zoology, Cambridge University, Cambridge CB2 3EJ, UK
† Departments of Physiology and ‡ Biological Chemistry, Minerva Center for Studies of Visual Transduction, The Hebrew University, Jerusalem 91010, Israel

PROTEIN kinase C (PKC) is a key enzyme for many cellular processes[1,2] but its physiological roles are poorly understood. An excellent opportunity to investigate the function of PKC has been provided by the identification of an eye-specific PKC in *Drosophila*[3–5] and a null PKC mutant, *inaC*^{P209} (refs 5,6). Bright conditioning lights delivered to *inaC* photoreceptors lead to an abnormal loss of sensitivity in whole cell recordings from dissociated ommatidia; this has been interpreted as 'hyper-adaptation' and PKC's role has been suggested to be distinct from light adaptation[5]. A presumably related finding is that during intense light, the response of *inaC* declines to baseline[6]. Invertebrate photoreceptors use the phosphoinositide signalling cascade[7–12], responding to single photons with so-called quantum bumps[13] which sum to form the macroscopic response to light[14–16]. Light adaptation allows photoreceptors to adjust their sensitivity over the enormous range of ambient intensities[14,17]. Although the molecular mechanism of light adaptation remains obscure, it is a negative-feedback process[12] mediated by a rise in cytosolic calcium[12,18] and a decrease in bump size[12,14–16]. We now show that under physiological conditions light adaptation is severely reduced in *inaC*, suggesting that eye-specific PKC, itself activated by a rise in cytosolic calcium[4,5] and diacylglycerol, is required for adaptation. Furthermore, we show that in the absence of PKC individual bumps fail to terminate normally, an effect that can account for the pleiotropic manifestations of the *inaC* phenotype.

Another mutant showing behaviour similar to *inaC* is the transient receptor potential mutant (*trp*). In *trp* this phenotype, which we refer to as response inactivation[19], is thought to represent exhaustion of the excitatory process[20,21], and in fact virtually all manifestations of light adaptation are lacking in this mutant[19–22]. The primary defect in *trp* is the absence of a light-activated Ca^{2+} channel[23,24], suggesting that inactivation reflects depletion of the inositol trisphophate ($InsP_3$)-sensitive calcium stores and that these require Ca^{2+} influx through the *trp*-dependent channels to be rapidly refilled. The measure previously used to assess 'adaptation' in *inaC* (decrease in response amplitude)[5] is common to both adaptation and inactivation[19]. Also, the inclusion of 10mM EGTA in excess of Ca^{2+} in the whole cell recording pipette[5] and removal of all Na^+ from the bathing solution[5] (thereby blocking Na^+/Ca^{2+} exchange) make measurement of Ca^{2+}-dependent light adaptation difficult. We re-examined *inaC* using criteria developed in *trp*[21] to distinguish the fundamentally different mechanisms of adaptation and response inactivation. Furthermore, as the dissociated ommatidia preparation is unstable during the prolonged illumination regimes required to measure adaptation, we made measurements under strictly physiological conditions using intracellular recordings from intact flies. An obvious manifestation of adaptation is the rapid transition from peak to plateau following the onset of bright light. In *inaC* this phase is missing[4,5]; instead, above a certain intensity, responses decay slowly to a low steady-state level (Fig. 1*a*, *d*), reaching baseline during intense white lights (data not shown). The classical, quantitative manifestation of light adaptation is a shift in the photoreceptor's operational range from dim to bright lights (V/log I curve)[17,25,26]. As in *trp*[21,27], we found virtually no shift in *inaC* photoreceptors with dim or moderate backgrounds which clearly cause adaptation in wild-type (WT) photoreceptors (Fig. 1*b*,*c*). The parameters characterizing the V/log I curve σ (expressing adaptational shift), and V_{max}, are clearly different in wild type and *inaC* (Fig. 1*c*), indicating that the reduction in

§ To whom correspondence should be addressed.